Progress in Biophysics and Molecular Biology 116 (2014) 11–24

Contents lists available at ScienceDirect

Progress in Biophysics and Molecular Biology

journal homepage: www.elsevier.com/locate/pbiomolbio

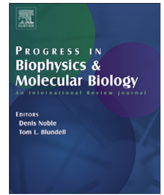

Original research

EAD and DAD mechanisms analyzed by developing a new human ventricular cell model

K. Asakura [b, 2], C.Y. Cha [a, 1, 2], H. Yamaoka [a], Y. Horikawa [a], H. Memida [a], T. Powell [c], A. Amano [a], A. Noma [a, *]

[a] *Biosimulation Project, College of Life Sciences, Ritsumeikan University, Japan*
[b] *Nippon Shinyaku, Co., Ltd., Kyoto, Japan*
[c] *Department of Pharmacology, University of Oxford, Oxford OX1 3QT, UK*

A R T I C L E I N F O

Article history:
Available online 1 September 2014

Keywords:
Human ventricular myocyte
Mathematical model
Early afterdepolarization
Delayed afterdepolarization
Late Na^+ current
Lead potential analysis

A B S T R A C T

It has long been suggested that the Ca^{2+}-mechanisms are largely involved in generating the early afterdepolarization (EAD) as well as the delayed afterdepolarization (DAD). This view was examined in a quantitative manner by applying the lead potential analysis to a new human ventricular cell model. In this ventricular cell model, the tight coupled LCC-RyR model (CaRU) based on local control theory (Hinch et al. 2004) and ion channel models mostly based on human electrophysiological data were included to reproduce realistic Ca^{2+} dynamics as well as the membrane excitation. Simultaneously, the Ca^{2+} accumulation near the Ca^{2+} releasing site was incorporated as observed in real cardiac myocytes. The maximum rate of ventricular repolarization (−1.02 mV/ms) is due to I_{K1} (−0.55 mV/ms) and the rest is provided nearly equally by I_{NCX} (−0.20 mV/ms), I_{NaL} (−0.16 mV/ms) and I_{NaT} (−0.13 mV/ms). These I_{NaL} and I_{NaT} components are due to closure of the voltage gate, which remains partially open during the plateau potential. DADs could be evoked by applying high-frequency stimulations supplemented by a partial Na^+/K^+ pump inhibition, or by a microinjection of Ca^{2+}. EADs was evoked by retarding the inactivation of I_{NaL}. The lead potential (V_L) analysis revealed that I_{K1} and I_{Kr} played the primary role to reverse the AP repolarization to depolarizing limb of EAD. I_{CaL} and I_{NCX} amplified EAD, while the remaining currents partially antagonized dV_L/dt. The maximum rate of rise of EAD was attributable to the rapid activation of both I_{CaL} (45.5%) and I_{NCX} (54.5%).

© 2014 Elsevier Ltd. All rights reserved.

1. Introduction

Two types of afterdepolarizations have been observed following a full-size action potential (AP) in isolated ventricular myocytes. One is the early afterdepolarization (EAD) and the other is delayed afterdepolarization (DAD) (Antzelevitch and Burashnikov, 2011; Fozzard, 1992; Volders et al., 1997). In both types of afterdepolarizations, the Ca^{2+} induced Ca^{2+} release (CICR) from sarcoplasmic reticulum largely modifies the membrane excitation through activation of inward I_{NCX}. Therefore, modeling CICR based on biophysical mechanisms has long been one of the critical issue to analyze both normal and abnormal electrical activities in cardiac myocytes (Greenstein and Winslow, 2002; Hinch, 2004; Hinch et al., 2004; Stern, 1992; Winslow et al., 1999, 2000). Recently, Hinch et al. (2004, 2006) largely innovated the model of CICR by defining an explicit Ca^{2+}-release unit (CaRU), and by applying a new algorithm for computing the CICR according to local control theory at a low computational cost. The present study adopted this Hinch model of CaRU.

Abbreviations: AP, action potential; EAD, early afterdepolarization; DAD, delayed afterdepolarization; APD_{90}, action potential duration measured at 90% repolarization; V_m, membrane potential; V_L, lead potential; I_{NaL}, late component of Na^+ current; F_b, cross-bridge force; SR, sarcoplasmic reticulum; CICR, Ca^{2+}-induced Ca^{2+} release from SR; LTCC, L-type Ca^{2+} channel; GPB model, human ventricular cell model developed by; I_{CaL}, L-type Ca^{2+} current; I_{Na}, V_m-dependent Na^+ current (I_{NaT} + I_{NaL}); I_{K1}, inward rectifier K^+ current; I_{Kr}, rapid component of delayed rectifier K^+ current; I_{Ks}, slow component of delayed rectifier K^+ current; I_{Kto}, transient outward K^+ current; I_{Kpl}, plateau K^+ current; $I_{l(Ca)}$, Ca^{2+}-activated background cation current; I_{Cab}, background Ca^{2+} current; I_{KATP}, ATP-sensitive K^+ current; I_{bNSC}, background non-selective cation current; I_{NCX}, Na^+/Ca^{2+} exchanger current; I_{PMCA}, plasma membrane Ca^{2+} ATPase current; I_{NaK}, Na^+/K^+ pump current; J_{SERCA}, Ca^{2+} flux of sarco-/endoplasmic reticulum Ca^{2+} pump.

* Corresponding author. Biosimulation Project, College of Life Sciences, Ritsumeikan University, Noji Higashi 1-1-1, Kusatsu-City, Shiga-prefecture 525-8577, Japan. Tel.: +81 77 561 2586.
E-mail address: noma@sk.ritsumei.ac.jp (A. Noma).
[1] Present address: Oxford Centre for Diabetes Endocrinology and Metabolism, University of Oxford, Churchill Hospital, Oxford, OX37 LJ, UK.
[2] K. Asakura and 'C.Y. Cha equally contributed to the present paper.

http://dx.doi.org/10.1016/j.pbiomolbio.2014.08.008
0079-6107/© 2014 Elsevier Ltd. All rights reserved.

The spontaneous Ca^{2+} release from SR might be triggered by a local Ca^{2+} accumulation near Ca^{2+} releasing sites, which has been well established in experimental studies (Acsai et al., 2011; Weber et al., 2001, 2002). This Ca^{2+} accumulation was reconstructed by optimizing the microscopic structure of the dyadic space to allow moderate interactions between the neighboring CaRUs in the present study. The contraction model of Negroni and Lascano (2008) was also incorporated in the cell model to constrain model adjustment of $[Ca^{2+}]$ variations in the bulk cytosolic space. The SR Ca^{2+} pump (SERCA) developed by Tran et al. (2009) was used to calculate Ca^{2+} uptake by the SR. The models of ionic currents in this study are extensions of previous models in human or animal cell models (Grandi et al., 2010; Iyer et al., 2004; O'Hara et al., 2011; Priebe and Beuckelmann, 1998; Takeuchi et al., 2006; ten Tusscher et al., 2004). The late component of I_{Na} (I_{NaL}) was also incorporated (Carmeliet, 1987; Coraboeuf et al., 1979; Gintant et al., 1984; Maltsev et al., 1998; Undrovinas et al., 1999) by developing a new Markovian-type channel gating scheme, since I_{NaL} may contribute to generation of EAD through pathophysiological retardation of its inactivation in human ventricular cells (Undrovinas et al., 1999). The new ventricular cell model revealed that the SR Ca^{2+} release is involved in EAD configuration as well as in DAD. Contributions of the dynamic activities of all ion channels and transporters to the EAD were quantified by conducting the lead potential analysis (Cha et al., 2009, 2011b).

2. Methods

The framework of our ventricular cell model is similar to that of human ventricular cell model developed by Grandi et al. (2010) (GPB model). The cytoplasm (V_{cyt}, i.e. a diffusion space of ions) was divided into three Ca^{2+} compartments: a junctional space (*jnc*), an intermediate zone (*iz*), and a bulk space (*blk*) as indicated with different colors in Fig. 1 (Table S3). The proportions of *blk* (65%) to the cell volume (V_{cell}) remain nearly the same as those in the GPB model. A steep diffusion gradient of $[Ca^{2+}]$ around the Ca^{2+} releasing site was divided into two discrete steps $[Ca^{2+}]_{jnc}$ and $[Ca^{2+}]_{iz}$. The *jnc* provides a direct sink for the Ca^{2+} fluxes through CaRUs. The volume of *jnc* was adjusted to 1.1% of the V_{cell}, which is about 11 time larger than assumed in GPB model. The *iz* (3.5% of V_{cell}) provides an intermediate zone between *jnc* and *blk*. The ion channels and transporters were distributed on the sarcolemma; LCC in *jnc*, $[Ca^{2+}]$-related currents in *iz* such as, LCC, I_{Ks}, I_{Cab}, $I_{L(Ca)}$, Na^+/Ca^{2+} exchanger (NCX), and PMCA, and all 11 kinds of channels and 3 types of transporters in *blk*. The SR space was divided into a Ca^{2+}-uptake site (SR_{up}) and a Ca^{2+}-releasing site (SR_{rl}), which represent 60% and 40% of the total SR space (3.5% of V_{cell}), respectively. SERCA is located on the membrane of SR_{up} and regulates both $[Ca^{2+}]_{blk}$ and $[Ca^{2+}]_{SRup}$.

The volume of *iz* (vol_{iz}) was determined based on electrophysiological measurement of I_{NCX} in the *nrs*-space, which is a space near the Ca^{2+} releasing site defined experimentally by Acsai et al. (2011). The peak of $[Ca^{2+}]_{nrs}$ transient was estimated to be 10–15 μM by comparing the peak I_{NCX} with the standard $[Ca^{2+}]$–I_{NCX} relationship. In the present model, a peak $[Ca^{2+}]_{iz}$ of ~9 μM was obtained with the vol_{iz} of 3.5% of V_{cyt}. According to the experimental recording of I_{NCX} evoked by the Ca^{2+} transient during 10- and 30-ms step pulses (simulated in Fig. S7A), a 10% fraction of NCX was located in *iz* and the rest in *blk*. The co-localization study (Scriven and Moore, 2013) revealed that NCXs are present on the T-tubule membrane, except dyads, while most LCCs are distributed in dyads. Therefore, we assumed a presence of 75% LCCs, but no NCX in *jnc*. This parameter determination also satisfied experimental measurement of Ca^{2+}-mediated inactivation of I_{CaL} with and without SR Ca^{2+} release (Fig. S7B).

The detailed set of Ca^{2+} buffer species described in the GPB model was adopted after a simplification ('Ca^{2+} buffering' and Table S6 in Supplemental materials). The low affinity binding of Ca^{2+} to troponin (TnCl) in the GPB model was replaced by a dynamic contraction model (Negroni and Lascano, 2008), and the

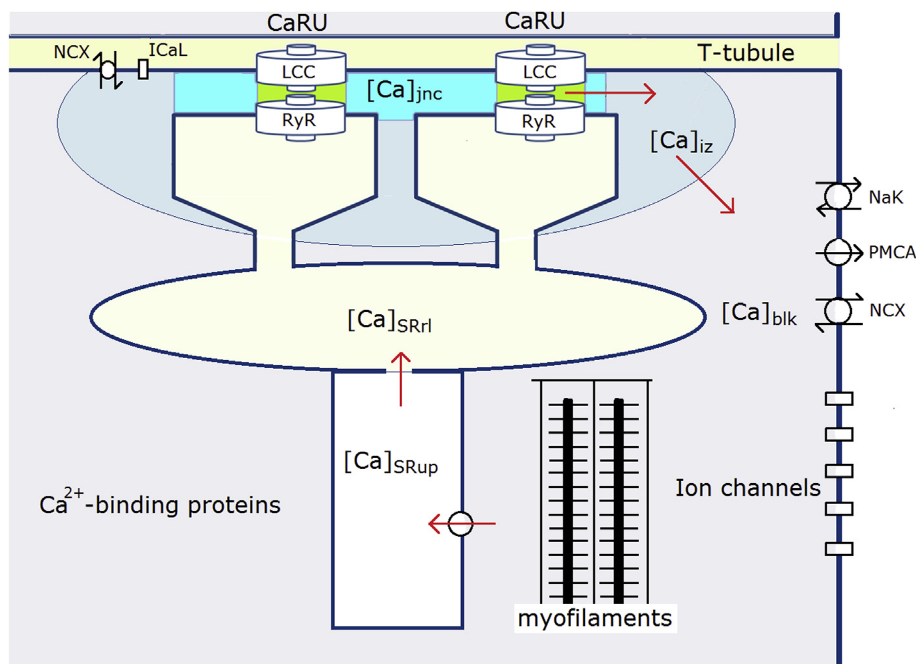

Fig. 1. Composition of the new human ventricular cell model represented by a half-sarcomere. The compartments of *jnc*, *iz*, and *blk* in the cytosol, SR_{up} and SR_{rl} of the SR and T-tubule are filled with different colors. The ion channels and transporters are located on the sarcolemma, SERCA, RyRs on the SR membrane and the contractile fibers within *blk*. A single CaRU consists of a L-type Ca^{2+} channel (LCC) and a RyR unit, which are separated by a nanodomain (filled with green color) between the two channel proteins, and is spatially separated from its neighbor CaRUs, though only two CaRUs are illustrated for simplicity. The nanodomain provides a pathway of Ca^{2+} influxes of LCC and RyR to *jnc*. Then, Ca^{2+} diffuses from *jnc* to *iz*, and to *blk* to be pumped up to SRup by SERCA as indicated by red arrows. The contraction model is from Negroni and Lascano (2008).

Download English Version:

https://daneshyari.com/en/article/2070529

Download Persian Version:

https://daneshyari.com/article/2070529

Daneshyari.com